Transactions of the Materials Research Society of Japan 29 [2] 615-618 (2004)

Magneto-optical Kerr Effect of Nickel Nanoparticles in SiO_2 Fabricated by Negative-ion Implantation of 60 keV

H. Amekura, Y. Takeda, K. Kono and N. Kishimoto
Nanomaterials Laboratory, National Institute for Materials Science
Fax: 81-29-863-5599, e-mail: amekura.hiroshi@nims.go.jp

Magneto-optical Kerr effects, i.e., Kerr rotation and Kerr ellipticity, of nickel nanoparticles in silica glasses (SiO_2) fabricated by implantation of Ni negative ions of 60 keV were studied by the optical-retardation modulation technique, in the photon energy region of 1.38 – 6.20 eV, under the magnetic field up to 21 kOe at room temperature. For comparison, those effects of Ni films (~120 nm thick) deposited on SiO_2 were also studied. Although the Kerr rotation signal of the nanoparticles was overlapped by strong Faraday rotation signal from the SiO_2 substrate, the ellipticity signal of the nanoparticles was hardly influenced. Although the Ni film shows a typical parallelogrammic Kerr loop with a hysteresis, the Ni nanoparticles show a gradual loop without hysteresis which is characteristic in superparamagnetic nanoparticles.

Key words: magnetic nanoparticle, magneto-optical Kerr effect, ion implantation, superparamagnetism, nickel

1. INTRODUCTION

Magnetic nanoparticles dispersed in insulators draw much attention, because of applicability for super high-density data storage [1] and tunneling magneto-resistance (TMR) devices [2], etc. High-flux negative-ion implantation is one of the most promising methods to fabricate metal nanoparticles in insulators, without heat treatment, with good controllability inherent in ion implantation and without surface charge accumulation [3]. Up to now, we have implanted Ni negative-ions of 60 keV to silica glasses (SiO_2), and confirmed the Ni nanoparticles formation (mean diameter of ~3 nm) in SiO_2 using cross-sectional transmission electron microscopy (TEM) [4]. However, detection of magnetization of the Ni nanoparticles was not easy, since the signal from the nanoparticles was overlapped by a strong signal from the matrix SiO_2. Although the diamagnetic signal per volume of the matrix SiO_2 is small, the volume fraction of the nanoparticles to the matrix is by far small. Applying a very long integration time, typically ~8 hours for a half of *M-H* loop ($0 < H < 50$ kOe), we have succeeded in detecting the superparamagnetic behaviors of the Ni nanoparticles using a SQUID magnetometer [5].

In this paper, an alternative method of magnetization evaluation, i.e., magneto-optical Kerr measurement is carried out. Although the Kerr measurement cannot determine an absolute value of the magnetization, a drastic reduction of measurement-time is expected, because of (i) selective detection of Ni nanoparticle magnetization with tuning adequate photon-energy and (ii) fast optical modulation. The fast optical modulation is contrast to the slow mechanical differential detection of the SQUID measurements. Moreover, information on interactions between light and magnetization, e.g., an off-diagonal component of complex dielectric function, can be obtained. The Kerr measurements are also applicable to high temperature measurements compared to the SQUID measurements.

2. EXPERIMENTALS

Two types of samples, namely Ni nanoparticles in SiO_2 and Ni thin-films (continuous films) on SiO_2 substrates, were used. The nanoparticles in SiO_2 was just fabricated by implantation of Ni negative-ions of 60 keV to SiO_2. The Ni nanoparticles were spontaneously formed in SiO_2 without any heat treatments [5].

The Ni films were deposited on virgin SiO_2 substrates by resistive heating. The base pressure was less than $\sim 1\times10^{-4}$ Pa. The film thickness of ~120 nm was determined by a step-height profiler (DEKTAK V200SI). Optical-grade silica glasses (KU-1: OH^- 820 ppm) of 15 mm in diameter and 0.5 mm in thickness were cut into four pieces of sectors, and were used for either the substrates of the ion implantation or those of the film evaporation.

Nickel negative-ions (Ni^-) from a Cs-assisted plasma-sputter type high-flux ion source [6] were used for the implantation. After mass separation, the Ni ions of 60 keV were implanted. The implanted area was 6 mm in diameter. The ion fluxes and the fluences ranged over 1 - 100 $\mu A/cm^2$ and 3×10^{16} -1×10^{17} ions/cm^2, respectively. The fluences were confirmed by the Rutherford Backscattering Spectrometry (RBS) using 2.06 MeV He^+ beam with a scattering angle of 160 degrees. In this paper, results of samples implanted with a flux of 56 $\mu A/cm^2$ and a dose of 3.8×10^{16} ions/cm^2 are shown. According to SRIM2000 code [7], the projectile range R_P and the straggling ΔR_P of Ni ions of 60 keV are 47 nm and 16 nm in SiO_2, respectively.

For magneto-optical Kerr measurements [8,9], the

sample was set between magnetic poles of an iron-core magnet. Magnetic field was applied normal to the sample surface up to ~21 kOe. The sample was illuminated by light from a 150 W Xe lamp via a 30 cm single grating monochromator through a hole on the magnetic pole, i.e., the polar Kerr configuration. A wavelength resolution of the monochromator was set in 1 nm. An incident angle of the light to the sample was 7 degrees from normal to the surface. Between the monochromator and the magnet, a polarizer and a photo-elastic modulator (PEM) were inserted to modulate the optical retardation of the incident light. The reflected light was collected by a photomultiplier via another polarizer.

The PEM modulated optical retardation $\delta = \delta_0 \sin pt$ of the incident light with a frequency p of ~42 kHz. Intensities of p-, $2p$- and DC components, $I(p)$, $I(2p)$ and $I(0)$, in the reflected light were obtained by a phase-sensitive detection. When the amplitude of the retardation δ_0 is kept as $J_0(\delta_0) = 0$, i.e., $\delta_0 = 2.4048$, the Kerr rotation θ_K and ellipticity η_K are given by

$$\theta_K = 0.5790\, I(2f)/I(0), \quad (1)$$

$$\eta_K = 0.4816\, I(f)/I(0), \quad (2)$$

where $J_0(x)$ denotes the 0-th order Bessel function [8,9]. Polarities of θ_K and η_K were determined from a standard $Pt_{60}Co_{40}$ alloy film (~50 nm thick) to reproduce results shown in Ref. [10]. This definition of the polarities is consistent with that proposed by IEEE [11]. However, it is different from those used in a series of studies on band calculations and experimental results of Kerr effect of Ni films [12-16].

Magneto-optical Kerr spectra, both the rotation spectra and the ellipticity spectra, were determined from Kerr loop measurements at fixed photon energies. At each of the fixed energies between 1.38 – 6.20 eV, the Kerr loops, i.e., field dependences of Kerr rotation or ellipticity, were measured with changing the field between -21 and 21 kOe.

3. RESULTS AND DISCUSSION

Figure 1 shows magneto-optical hysteresis loops of a Ni film on SiO_2 substrate and of Ni nanoparticles in SiO_2. The Ni film was illuminated from the film surface side, not from the substrate side. Both the rotation and the ellipticity show typical parallelogrammic loops which are characteristic in ferromagnetic materials. A field required for the magnetization saturation H_s was ~4 kOe, which is much higher than the value of bulk Ni (less than 0.2 kOe [17]). However, the high saturation field H_s is due to the large demagnetization field from the measurement configuration where the field is applied normal to the film surface. The rotation θ_K (curve (a)) slightly decreases in higher field than $\pm H_s$, although η_K (curve (b)) keeps a constant value in higher field. The decrease is probably due to the Faraday rotation of SiO_2 substrate. Although the transmission of light through the Ni film of ~120 nm thick is very low, a small portion of the transmitted light induces the large Faraday rotation.

Curve (c) shows a Kerr rotation loop of Ni nanoparticles in SiO_2. The loop is dominated by a strong

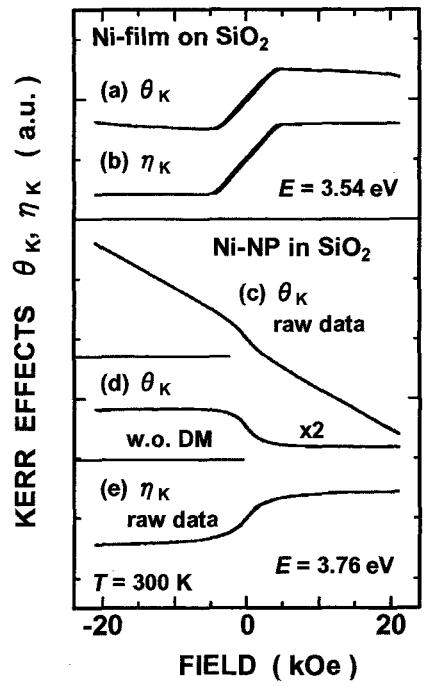

Fig.1 Magneto-optical hysteresis loops of a Ni film on SiO_2 substrate (upper part) and Ni nanoparticles in SiO_2 (lower part) detected as Kerr rotation θ_K (curves (a) and (c)) and ellipticity η_K (curves (b) and (d)). The loop (d) was obtained after reduction of a diamagnetic component from the loop (c).

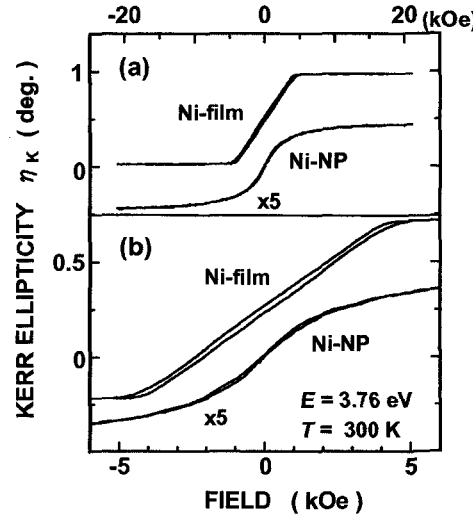

Fig.2 Hysteresis loops of a Ni film on SiO_2 substrate and Ni nanoparticles in SiO_2 detected by Kerr ellipticity η_K. The low field region of the loops shown in Fig. 2(a) is magnified and shown in Fig. 2(b).

linear component against the field with a negative slope. Since the linear component shows a photon energy dependence which is completely different from the Ni signal but similar to the unimplanted SiO_2, the linear component is ascribed to the Faraday rotation of SiO_2. It should be noted that Kerr rotation of SiO_2 is very small,

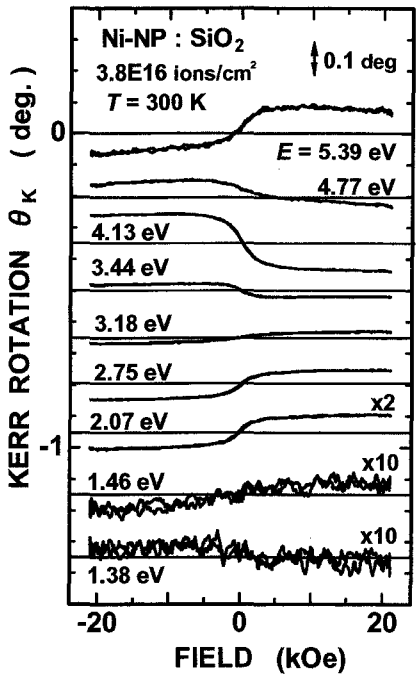

Fig.3 Kerr rotation loops of Ni nanoparticles in SiO_2 detected at several photon energies at T = 300 K. The linear components from the Faraday rotation due to SiO_2 were excluded. One division of ordinate corresponds to 0.1 degrees.

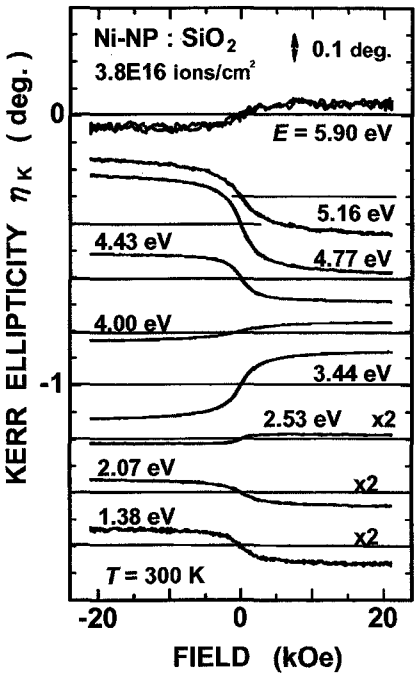

Fig.4 Kerr ellipticity loops of Ni nanoparticles in SiO_2 detected at several photon energies at T = 300 K. One division of ordinate corresponds to 0.1 degrees.

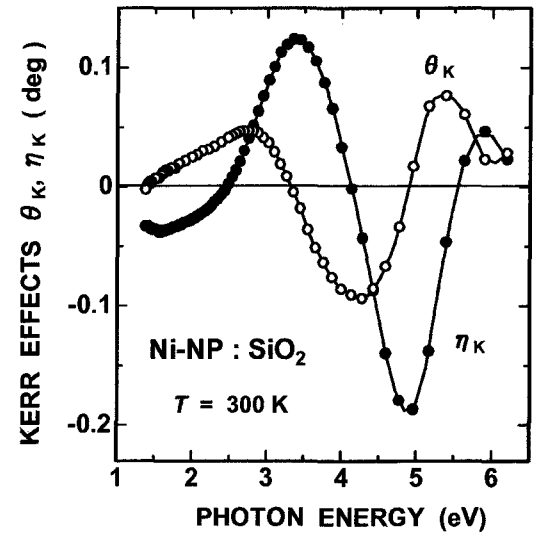

Fig.5 Kerr rotation (open circles) and ellipticity (closed circles) spectra of Ni nanoparticles in SiO_2 determined from the loops at each wavelength at T = 300 K. In the rotation spectra, linear components due to the Faraday rotation of SiO_2 substrate were excluded.

because SiO_2 is not ferromagnetic. The superposition of Kerr rotation from Ni nanoparticles and Faraday rotation from SiO_2 substrate is observed, because the sample shows a brownish but transparent color. The incident light efficiently interacts with not only Ni nanoparticles but also the SiO_2 substrate. The Kerr rotation component of Ni nanoparticles was obtained by subtraction of the linear component, as shown in curve (d). However, this procedure limits S/N ratio and reliability of Kerr rotation measurements. Curve (e) shows a Kerr ellipticity loop of the nanoparticles in SiO_2. Since the Faraday ellipticity effect of SiO_2 is very weak in UV-VIS region, the ellipticity measurements are almost free from the substrate contribution.

Figure 2 shows comparison of a Kerr ellipticity loop of the film and that of the nanoparticles. The film shows a parallelogrammic loop with hysteresis which is characteristic in ferromagnetic materials. The coercive field was in ~0.18 kOe. Contrarily, the nanoparticles show a smooth and slow-rising curve which is characteristic in superparamagnetic particles [5]. Within an experimental error, hysteresis was not observed.

Kerr rotation and ellipticity loops of Ni nanoparticles in SiO_2 were measured at T = 300 K, from 1.38 to 6.20 eV in the photon energy. In the rotation loops, the linear components from the Faraday rotation of SiO_2 were excluded. Examples of the loops at several photon energies are shown in Fig. 3 for the rotation and in Fig. 4 for the ellipticity, respectively. The loop changes with the photon energy, not only in the magnitude, but also in the polarity.

The wavelength dependence of θ_K and η_K at H = 21 kOe are summarized in Fig. 5. The spectra of rotation and ellipticity should be connected to each other by the Kramers-Kronig relationship; the S-shaped dispersion in η_K corresponds to the bell-type spectral

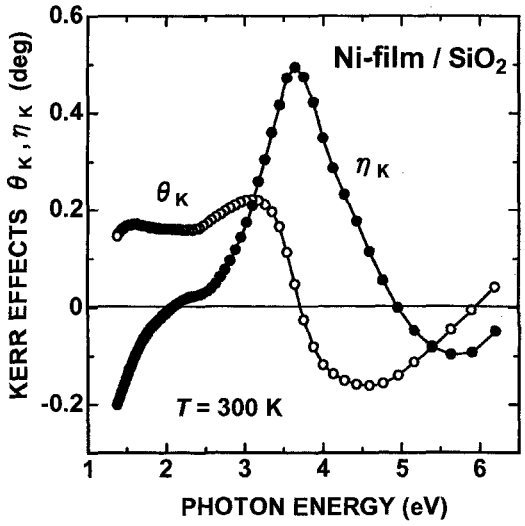

Fig.6 Kerr rotation (open circles) and ellipticity (closed circles) spectra of a Ni film (~120 nm thick) on SiO_2 substrate determined from the loops at each wavelength at T = 300 K. In the rotation spectra, linear components from the Faraday rotation due to SiO_2 substrate were excluded.

shape of θ_K with side wings of opposite sign. This is exactly observed in Fig. 5, where the center of dispersion in η_K at ~4 eV coincides with the negative peak of θ_K.

Using the same method to obtain Fig. 5, Kerr rotation and ellipticity spectra of Ni film were obtained, and shown in Fig. 6. The spectra of Ni film (Fig. 6) are different from the spectra of Ni nanoparticles in SiO_2 (Fig. 5). This is because Ni nanoparticles in SiO_2 should be regarded as *a composite*: Optical and magneto-optical properties of the nanoparticle composite are determined from a dielectric function (tensor) of the composite, which is determined from dielectric function (tensors) of Ni and SiO_2 via complex relations, e.g., the Maxwell-Garnett formula or the extensions [18]. Relationship between the Kerr spectra of Ni film and those of Ni nanoparticles in SiO_2 will be discussed elsewhere.

4. CONCLUSIONS

Magneto-optical Kerr effects (Kerr rotation and ellipticity) of nickel nanoparticles in silica glasses (SiO_2) fabricated by implantation of Ni negative-ions of 60 keV were studied by the optical-retardation modulation technique using a photo-elastic modulator, in the photon energy region of 1.38 – 6.20 eV, under the magnetic field up to 21 kOe at room temperature. For comparison, those effects of Ni films (~120 nm thick) deposited on SiO_2 were also studied. Although the Kerr rotation signal of the nanoparticles was overlapped by strong Faraday rotation signal from the substrate SiO_2, the ellipticity signal of the nanoparticles was hardly influenced. The Ni film shows a typical parallelogrammic Kerr loop with a hysteresis. The coercive field was 0.18 kOe. The nanoparticles show a slow-rising loop without hysteresis which is characteristic in superparamagnetic nanoparticles.

ACKNOWLEDGMENTS

A part of this study was financially supported by the Budget for Nuclear Research of the MEXT, based on the screening and counseling by the Atomic Energy Commission.

REFERENCES

[1] For example, C.B. Murray, S. Sun, H. Doyle and T. Betley, *MRS-Bull.*, **26**, 985-991 (2001).
[2] J.I. Gittleman, Y. Goldstein and S. Bozowski, *Phys. Rev.*, **B5**, 3609-3621 (1972).
[3] J. Ishikawa, H. Tsuji, Y. Toyota, Y. Gotoh, K. Matsuda, M. Tanjyo and S. Sakaki, *Nucl. Instr. and Meth.*, **B96**, 7-12 (1995).
[4] H. Amekura, N. Umeda, Y. Takeda, H. Kitazawa and N. Kishimoto, *Trans. Mat. Res. Soc. Jpn.*, **28**, 465-468 (2003).
[5] H. Amekura, H. Kitazawa, T. Mochiku, N. Umeda, Y. Takeda and N. Kishimoto, *Proc. of SPIE*, **4936**, 1-8 (2002).
[6] N. Kishimoto, Y. Takeda, V.T. Gritsyna, E. Iwamoto and T. Saito, "IEEE Transactions from 1998 International Conference on Ion Implantation Technology Proceedings", Ed. By J. Matsuo, G. Takaoka and I. Yamada, IEEE, Piscataway (1999) pp. 342-345.
[7] J.F. Ziegler, J.P. Biersack and U. Littmark, "The Stopping and Range of Ions in Solids", Pergamon press, New York (1985) Chap.8. http://www.srim.org/.
[8] K. Sato, *Jpn. J. Appl. Phys.*, **20**, 2403-2409 (1981).
[9] K. Sato, H. Hongu, H. Ikekame, Y. Tosaka, M. Watanabe, K. Takanashi and H. Fujimori, *Jpn. J. Appl. Phys.*, **32**, 989-995 (1993).
[10] K. Sato, H. Hongu, H. Ikekame, J. Watanabe, K. Tsuzukiyama, Y. Togami, M. Fujisawa and T. Fukuzawa, *Jpn. J. Appl. Phys.*, **31**, 3603-3607 (1992).
[11] "IEEE Standard Dictionary of Electrical and Electronical Terms", 3rd ed. IEEE (1984) p. 483, 789.
[12] S. Visnovsky, V. Parizek, M. Nyvlt, P. Kielar, V. Prosser and R. Krishnan, *J. Magn. Magn. Mater.*, **127**, 135-139 (1993).
[13] T. Gasche, M.S.S. Brooks and B. Johansson, *Phys. Rev.* **B53**, 296-301 (1996).
[14] N. Mainkar, D.A. Browne and J. Callaway, *Phys. Rev.* **B53**, 3692-3701 (1996).
[15] A. Delin, O. Eriksson, B. Johansson, S. Auluck and J.M. Wills, *Phys. Rev.* **B60**, 14105-14113 (1999).
[16] J. Kunes and P. Novak, *J. Phys.: Condens. Matter.*, **11**, 6301-6309 (1999).
[17] C. Kittle, "Introduction to solid state physics", 5th ed., John Wiley & Sons, New York (1976) Chap. 15.
[18] P.H. Lissberger and P.W. Saunders, *Thin Solid Films*, **34**, 323-333 (1976).

(Received October 9, 2003; Accepted January 20, 2004)